Available online at www.sciencedirect.com

ScienceDirect

Developmental Biology 303 (2007) 814–824

DEVELOPMENTAL BIOLOGY

www.elsevier.com/locate/ydbio

Genomes & Developmental Control

Activity-dependent neuroprotective protein (ADNP) differentially interacts with chromatin to regulate genes essential for embryogenesis

Shmuel Mandel [a], Gideon Rechavi [b], Illana Gozes [a,*]

[a] *Department of Human Molecular Genetics and Biochemistry, Tel Aviv University, Tel Aviv 69978, Israel*

[b] *Cancer Research Center, The Chaim Sheba Medical Center, Sackler Medical School, Tel Aviv University, Tel Aviv 69978, Israel*

Received for publication 3 September 2006; accepted 21 November 2006

Available online 1 December 2006

Abstract

Complete deficiency in activity-dependent neuroprotective protein (ADNP) results in neural tube closure defects and death at days 8.5–9.5 of gestation in the mouse (E8.5–9.5). To elucidate ADNP associated pathways, Affymetrix 22,690-oligonucleotide-based microarrays were used on ADNP knockout and control mouse embryos (E9) separated completely from extra embryonic tissue. Marked differences in expression profiles between ADNP-deficient embryos and ADNP-expressing embryos were discovered. Specifically, a group of dramatically up-regulated gene transcripts in the ADNP-deficient embryos were clustered into a family encoding for proteins enriched in the visceral endoderm such as apolipoproteins, cathepsins and methallotionins. In contrast, a down regulated gene cluster associated with ADNP-deficiency in the developing embryo consisted of organogenesis markers including neurogenesis (*Ngfr*, *neurogenin1*, *neurod1*) and heart development (*Myl2*). The pluripotent P19 cells were used for ADNP-chromatin-immunoprecipitation, showing direct interactions with multiple relevant gene promoters including members of the up-regulated as well as the down-regulated gene clusters. A comparison between non-differentiated and neuro-differentiated P19 cells revealed increased chromatin interaction of ADNP with chromatin from differentiated cells. These results place ADNP at a crucial point of gene regulation, repressing potential endoderm genes and enhancing genes associated with organogenesis/neurogenesis.

Keywords: ADNP; Gene array; Chromatin immunoprecipitation; P19; Visceral endoderm; Organogenesis/neurogenesis; Knockout embryos

Introduction

Activity-dependent neuroprotective protein (ADNP) is a 9 zinc finger, homeodomain containing protein possessing a putative transcription factor activity that was discovered in our laboratory (Bassan et al., 1999; Zamostiano et al., 2001). The ADNP homeodomain shows high similarity to the homeobox domain of the HOX protein family (USCA, Genome database), DNA-binding factors that are known to be involved in the transcriptional regulation of key developmental processes (Hombria and Lovegrove, 2003). ADNP contains a nuclear localization signal, as well as cellular export and import signals suggesting nuclear, cytoplasmic and extracellular functions (Furman et al., 2004; Gozes, 2001; Zamostiano et al., 2001).

ADNP is highly conserved in human, mouse and rat (Bassan et al., 1999; Sigalov et al., 2000; Zamostiano et al., 2001) and is overexpressed in malignant cells (Zamostiano et al., 2001). Expression of ADNP in mouse embryos was first detected at gestational day E7.5, peaked at E9, and reached its basal constitutive levels thereafter (Pinhasov et al., 2003; Poggi et al., 2002). Whole mount in situ hybridization showed high expression of ADNP in the developing embryonic brain and nervous system as well as lower expression in the rest of the embryonic body (Pinhasov et al., 2003).

Previous work has shown that ADNP acts as a vasoactive intestinal peptide (VIP) responsive gene (Bassan et al., 1999; Gozes et al., 2000; Pinhasov et al., 2003; Zusev and Gozes, 2004) and that VIP regulates embryonic development (Gressens et al., 1993; Hill et al., 1999). VIP has been shown to enhance the release of ADNP from glial cells (Furman et al., 2004) and in turn recombinant ADNP was shown to produce cellular

* Corresponding author. The Lily and Avraham Gildor Chair for the Investigation of Growth Factors Head, the Dr. Diana and Zelman Elton (Elbaum) Laboratory for Molecular Neuroendocrinology Sackler Faculty of Medicine Tel Aviv University, Tel Aviv 69978, Israel. Fax: +972 3 640 8541.

E-mail address: igozes@post.tau.ac.il (I. Gozes).

0012-1606/$ - see front matter © 2006 Elsevier Inc. All rights reserved.
doi:10.1016/j.ydbio.2006.11.039

protection against severe oxidative stress (Steingart and Gozes, 2006). An important neuroprotective active site on ADNP is a short eight amino acid peptide termed NAP (NAPVSIPQ) (Gozes et al., 2005) that provides neuroprotection through interaction with microtubules (Divinski et al., 2006). During embryonic development, NAP was shown to enhance neural tube closure that is inhibited by alcohol exposure (Chen et al., 2005).

To understand the physiological significance of ADNP, knockout mice were developed which showed marked growth retardation with E9.0 ADNP knockout (KO) embryos exhibiting an E8.0 phenotype. Furthermore, neural tube closure was inhibited in the ADNP KO embryos and at embryonic day 9.5 (E9.5), in utero absorption took place (Pinhasov et al., 2003). During mouse embryogenesis, the period from E8.5 to 10.5 encompasses a series of major developmental events. These include formation of the neural tube, the central nervous system primordium, which initiates at the cervical–hindbrain boundary at E8.5 and is completed at E10.5 following closure of the posterior neuropore. Other events during this interval include axial rotation, formation of differentiated somites, extensive remodeling of the heart with onset of regular contractions and placental chorioallantoic development (Greene et al., 2002). Previous studies have shown that during this stage of ontogeny, ADNP has a regulatory effect on genes such as PAX6 and OCT4 that are crucial for the development of the nervous system and for the maintenance of stem cells, respectively (Pinhasov et al., 2003). However, the mechanism by which ADNP exerts its vital developmental effects remains unknown.

In this study, we set out to elucidate the pathways involving ADNP activities during embryonic development and neurogenesis utilizing Affymetrix 22,690-oligonucleotide-based microarrays. Two model systems were used: the ADNP knockout mice and the model P19 cell line that can differentiate into neuronal-like cells. The results indicate dual participation for ADNP in the repression of a large set of genes that are associated with extra-embryonic tissues and in the enhancement of the expression of multiple genes associated with organogenesis, which enable proper embryonic development.

Materials and methods

Embryo dissections

All procedures involving animals have been approved by the Animal Care and Use Committee Tel Aviv University. ADNP heterozygous mice were checked for plug every 3 h. Plug day was assigned as day 0 (E0). A definitive determination of the developmental stage of each embryo at the time of harvesting was based on Theiler stages as before (Pinhasov et al., 2003). E9 whole embryos were separated from the extra embryonic tissue (yolk sac and amnion), immersed in ice-cold magnesium- and calcium-free phosphate-buffered saline, snap-frozen in liquid nitrogen, and stored at −80 °C until analysis. The extra embryonic tissue was stored separately and used for genotyping.

Primers

Primer pairs were designed using the primer 3 web interface (Rozen and Skaletsky, 2000) and synthesized by Sigma-Genosys (The Woodlands, TX). Primer sequences are shown in Table 1.

Genotyping and RNA extraction

To determine the embryonic genotype, DNA was extracted from embryonic yolk sacs and subjected to polymerase chain reaction (PCR) as described (Zusev and Gozes, 2004) using the neomycin and ADNP primers (Table 1). Two embryos from the same genotype and gestational time were pooled and RNA was isolated using Qiagene RNeasy mini kit (Qiagene, Hilden, Germany). Because of the small amounts of RNA extracted from one embryo at age E9 (~1.5 μg) a two embryo pool comprised of littermates possessing the same genotype was used. For comparative experiments all embryos were at approximately the same age. The same RNA extraction procedure was used on tissue culture cells.

Gene array

All experiments were performed using Affymetrix MOE430A oligonucleotide arrays, as described at http://www.affymetrix.com/products/arrays/specific/mouse430a_2.affx. Total RNA from each sample was used to prepare biotinylated target RNA, with minor modifications from the manufacturer's recommendations (http://www.affymetrix.com/support/technical/manual/expression_manual.affx).

Briefly, 3–5 μg of mRNA was used to generate first-strand cDNA by using a T7-linked oligo(dT) primer. After second-strand synthesis, in vitro transcription was performed with biotinylated UTP and CTP (Enzo Diagnostics), resulting in approximately 100-fold amplification of RNA. A complete description of procedures is available at: http://bioinf.picr.man.ac.uk/mbcf/downloads/GeneChip_Target_Prep_Protocol_CRUK_v_2.pdf.

The target cDNA generated from each sample was processed according to manufacturer's recommendation using an Affymetrix GeneChip Instrument System (http://www.affymetrix.com/support/technical/manual/expression_manual.affx). Briefly, spike controls were added to 10 μg fragmented cDNA before overnight hybridization. Arrays were then washed and stained with streptavidin–phycoerythrin, before being scanned on an Affymetrix Gene Chip scanner. A complete description of these procedures is available at http://bioinf.picr.man.ac.uk/mbcf/downloads/GeneChip_Hyb_Wash_Scan_Protocol_v_2_web.pdf Additionally, quality and amount of starting RNA was confirmed using an agarose gel. After scanning, array images were assessed by eye to confirm scanner alignment and the absence of significant bubbles or scratches on the chip surface. 3′/5′ ratios for GAPDH and beta-actin were confirmed to be within acceptable limits (0.8–0.88), and BioB spike controls were found to be present on all the arrays, with BioC, BioD and CreX also present in increasing intensity. When scaled to a target intensity of 100 (using Affymetrix MAS 5.0 array analysis software), scaling factors for all arrays were within acceptable limits (0.607–0.982), as were background, Q values and mean intensities. Details of quality control measures can be found (after publication of this article) at http://www.ncbi.nlm.nih.gov/geo/query/acc.cgi?=GSE4068.

Array analysis

In order to identify genes that were expressed differentially between the three genotypes, we used the Expander analysis software. Before applying the test, intensity levels below 20 were excluded (to reduce identification of changes at the noise level), and probes flagged as absent filtered out from the analyzed data. Functional and promoter analysis also used the Expander software (Sharan et al., 2003) and PRIMA program (Elkon et al., 2003).

Quantitative real time RT-PCR

Confirmatory quantitative gene-specific RT-PCR was performed using specific primers (Table 1). Total RNA was independently extracted from WT and ADNP null embryos using Qiagene RNeasy mini kit (Qiagene, Hilden, Germany), treated by *DNase*I (Ambion, Ausin, TX) and 1 μg RNA/sample was reverse-transcribed by SuperScript III reverse transcriptase (200 U, Invitrogene, Carlsbad, CA) using oligo(dT)20 primers (1 h at 50 °C, 5 min at 85 °C). Real-time RT-PCR was performed using FastStart DNA Master SYBR Green 1 dye-base detection kit (Roche Diagnostics Manncheim, Germany). We used the Light Cycler instrument with its internal relative quantification software (Roche

Table 1

Primer	Sequence	Annealing temperature	Size of product
ADNP (genomic)	5′ GTCCGTTACAGATTGTAC 3′ 5′ CTGCAGCAAAACAACTAT3′	51 °C	382
ADNP (for Real time PCR)	5′ CGAAAAATCAGGACTATCGG 3′ 5′ TGAAAGTGCTGAGGCTGCTA3′	60 °C	240
Neomycin	5′ ATGAATCCAGAAAAGCGGC 3′ 5′ ATCTCCTGTCATCTCACCT3′	57 °C	290
Neurogenine1	5′-GACACTGAGTCCTGGGGTTC-3′ 5′-GGCCTAGTGGTATGGGATGA-3′	60 °C	191
NeuroD1	5′-TGACCTTTCCCATGCTGAAT-3′ 5′-AAGTGCTAAGGCAACGCAAT-3′	60 °C	213
Galanin (*Gal*)	5′-TCATTTAGCGACAAGCATGG-3′ 5′-CAGTGGACATGGTCTCAGGA-3′	60 °C	232
Myosin light chain 2 (*Myl2*)	5′-GACCCAGATCCAGGAGTTCA-3′ 5′-ATTGGACCTGGAGCCTCTTT-3′	60 °C	162
Nerve growth factor receptor (*Ngfr*)	5′-TTTTGCTTGCTGTTGGAATG-3′ 5′-AAATACCACCGAGCACAAGG-3′	60 °C	150
Apolipoprotein E (*ApoE*)	5′-GGTTCGAGCCAATAGTGGAA-3′ 5′-TATTAAGCAAGGGCCACCAG-3′	60 °C	209
ApolipoproteinA1 (*apoA1*)	5′-GTGGCTCTGGTCTTCCTGAC-3′ 5′-ACGGTTGAACCCAGAGTGTC-3′	60 °C	218
Cathepsin L (*CtsL*)	5′-GTGGACTGTTCTCACGCTCA-3′ 5′-TATCCACGAACCCTGTGTCA-3′	60 °C	410
Cathepsin Z (*CtsZ*)	5′-CACCAGGACCAGGCTGTTAT-3′ 5′-CTTGTAGGTGCTGGTCACGA-3′	60 °C	150
Metallothionei1 (*Mt1*)	5′-ACCTCCTGCAAGAAGAGCTG-3′ 5′-GCTGGGTTGGTCCGATACTA-3′	60 °C	159
SerpinF2	5′-CAAGCTTAGACTGGCCTTGG-3′ 5′-GAGGAAGACTCCTGGCAGTG-3′	60 °C	160
L19	5′-CTGAAGGTCAAAGGGAATGTG-3′ 5′-GGACAGAGTCTTGATGATCTC-3′	60 °C	580
Actin	5′-TGTTACCAACTGGGACGACA-3′ 5′-GGGGTGTTGAAGGTCTCAAA-3′	60 °C	165
Metallothionein-I promoter	5′-AGCCCCCTCAGGAGTAGAGA-3′ 5′-CTCCAGCCCACGCATAGT-3′	60 °C	434
apoE promoter	5′-GGGAGAGAACAACCCGCC-3′ 5′-GGATCCCAGACCGGTCCA-3′	60 °C	105
CtsC promoter	5′-TGTCAACCCTGTATTGCACAG-3′ 5′-TTCAACTGGAACACCACTCG-3′	60 °C	400
Ctsz promoter	5′-ATGACCCACACCTTCTTCCA-3′ 5′-GCCCAAGTTGGACACACC-3′	60 °C	383
Myl2 promoter	5′-TTCCTCTTCCTCTCCCCTTC-3′ 5′-CCCCTGCTGTGGAACAATAA-3′	60 °C	404
Neurogn1 promoter	5′-CGACATCACTCAGGAGACCA-3′ 5′-TTCGAAGCGCACTTACTGTC-3′	60 °C	160
L19 promoter	5′-AGAGGACCACGTGACCAAAC-3′ 5′-CGAAAGGAAAGAGCTTGTGG-3′	60 °C	232

Diagnostics Manncheim, Germany), which utilizes melting point analysis to assess the specificity of the amplified genes. All reactions were performed with a magnesium chloride concentration of 2.5 mM, primer concentrations of 0.5 μM, and 2.5 μl of the reverse transcription product in a 10 μl reaction mixture. Annealing temperature was 60 °C for all genes checked. Relative quantification was performed by normalized ratio of ADNP-to-actin expression. Size was verified by melting curve analysis and agarose gel electrophoresis.

P19 cells

Embryonic carcinoma cells were obtained from the American Type Culture Collection (ATCC, Bethesda, MD); an initial control batch was a kind gift of Dr. Roi Atlas and Professor Irith Ginzburg. To induce neural differentiation, 1×10^6 aggregated P19 cells were cultivated in 90 mm bacteriological grade dishes in 10 ml of alpha-MEM containing 10% fetal calf serum, 100 units/ml penicillin and 100 mg/ml streptomycin (Biological Industries, Beit Haemek, Israel) in an incubator with 5% CO_2/37 °C and 1 μM *all–trans* retinoic acid (RA; Sigma, St. Louis, MO) for 4 days as described previously (Akiyama et al., 2003). Cell aggregates were suspended with trypsin-C (Biological Industries Beit Haemek, Israel) and transferred to tissue culture dishes. The cells were cultivated in RA free alpha-MEM containing 10% fetal calf serum for additional 4 days to induce neuronal and astroglial phenotype. All RNA extractions and real time PCR procedures were preformed on the P19 cells before, during and after retinoic acid-induced-differentiation.

Antibodies

Rabbit polyclonal anti C-terminal-ADNP (BL1034) were obtained from Bethyl Laboratories (Montgomery, TX). Rabbit polyclonal antibodies created in our laboratory against the hADNP epitops 1087–1101 and 185–199—anti C-terminal-ADNP (anti 79) and anti N-terminal-ADNP (anti 70) respectively (Miri Holtser-Cochav, Karin Vered and Illana Gozes, unpublished results). A purified IgG fraction was prepared by using AffinityPak prepacked columns of immunopure plus immobilized protein A (Pierce, Rockford, IL). Other

antibodies included, mouse monoclonal anti C-terminal-ADNP—(#612512, BD Biosciences, Franklin Lakes, NJ), rabbit polyclonal anti HP1α (Sigma, St. Louis, MO) and non-specific IgG from rabbit serum-(#15006, Sigma, St. Louis, MO), beta 3 tubulin as before (Divinski et al., 2006) and non-specific IgG from rabbit serum-(#15006, Sigma, St. Louis, MO). Secondary antibodies were goat anti-mouse-HRP (Jackson ImmunoResearch, West Grove, PA), goat anti-rabbit-HRP (Sigma St. Louis, MO) and HRP protein-A (Amersham Biosciences, Buckinghamshire, UK).

Chromatin immunoprecipitation assay

The chromatin immunoprecipitation (ChIP) assay was carried out following published protocols (Wells and Farnham, 2002) with slight modifications. In brief, P19 cells were cross-linked with formaldehyde (1% final concentration) for 10 min. All further manipulations were carried out at 4 °C. Cells were rinsed with PBS and lysed in SDS lysis buffer (1% SDS, EDTA 10 mM, Tris–HCl pH 8.1, 1× protease inhibitor cocktail (Sigma St. Louis, MO), for 30 min. The lysates were then re-suspended and chromatin was sonicated to an average DNA length of 500–1000 bp and then centrifuged at 16,000×*g* for 10 min. The supernatants were collected and diluted 10-fold in 0.01% SDS, 1% Triton X-100, 1.2 mM EDTA , 16.7 mM Tris HCl, pH 8.1, 167 mM NaCl with protease inhibitors (Sigma, St. Louis, MO) and subjected to immunoprecipitation with rabbit anti ADNP (Bethyl, anti 79 or anti 70 as described above) or non-specific rabbit IgG for 16 h. Immunocomplexes were collected by adsorption onto 25 µl protein A/G sepharose beads (Santa Cruz Biotechnologies, Santa Cruz, CA) for 16 h. The beads were washed sequentially with low salt wash buffer (0.1% SDS, 1% Triton X-100, 2 mM EDTA, 20 mM Tris–HCl, pH 8, and 150 mM NaCl), high salt wash buffer (0.1% SDS, 1% Triton X-100, 2 mM EDTA, 20 mM Tris–HCl, pH 8, and 500 mM NaCl), lithium chloride wash buffer (500 mM LiCl, 1% Nonidet P-40, 1% sodium deoxycholate, and 100 mM Tris–HCl, pH 8). Precipitates were washed with TE buffer (10 mM Tris–HCl, pH 8, 1 mM EDTA), and antibody-bound chromatin fragments were eluted from the beads with 1% SDS in 10 mM $NaHCO_3$. Cross-links were reverted by heating at 65 °C overnight. DNA was recovered using phenol chloroform DNA precipitation and analyzed for specific gene promoter sequences by PCR (as described above). ChIP DNA was amplified using 27–30 cycles. Primers used for analysis are listed in Table 1. The amplification product generated by each primer set is located within 300 bases of the putative initiation site of RNA transcription, as determined by sequence information available on the NCBI and UCSC genomic databases.

ADNP, HP1α coimmunoprecipitation

Nuclear proteins were extracted from P19 cells using Pierce NE-PER nuclear extraction buffer (Pierce, Rockford, IL) according to the manufacturer's protocol and supplemented with protease inhibitors cocktail (Sigma St. Louis, MO). Nuclear proteins were used for ADNP/ HP1α immunoprecipitation, using anti ADNP (Bethyl, Montgomery, TX), HP1α (Upstate, Lake Placid, NY) or non-specific rabbit IgG antibodies. 2 µg of each of the antibodies was added to P19 nuclear extracts and the sample was rotated

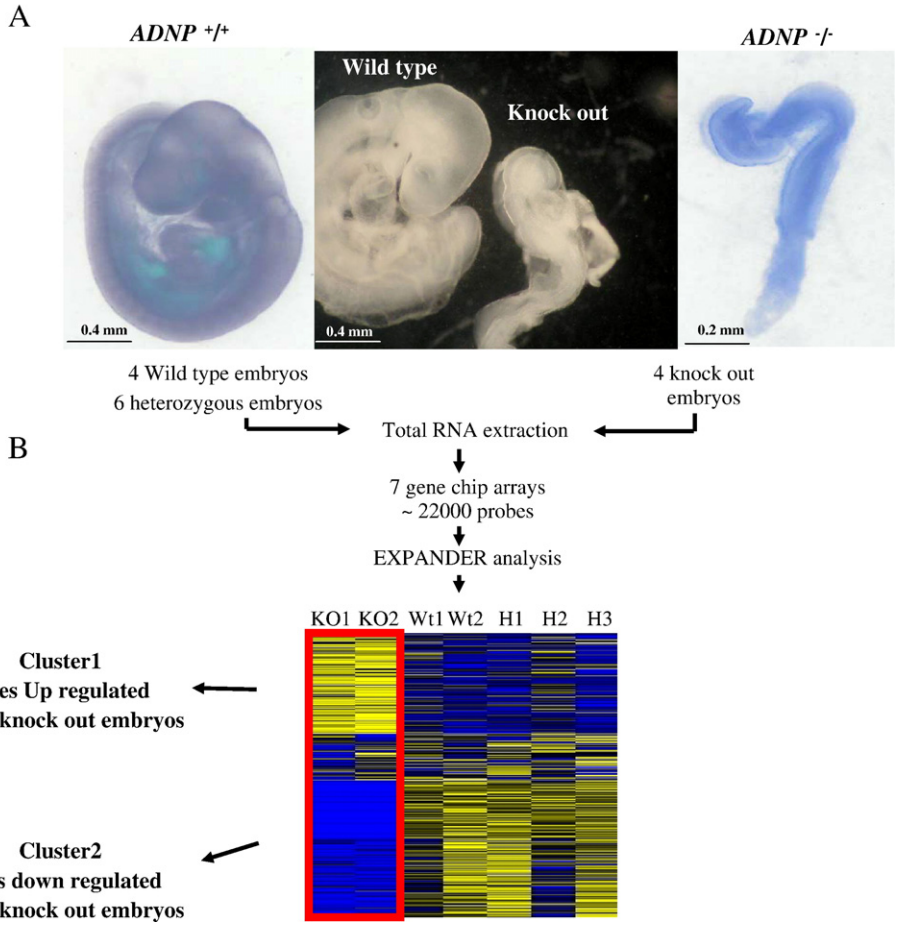

Fig. 1. ADNP-deficiency morphologic and genetic analysis. (A) Morphology of E9–9.5 wild type (WT = ADNP+/+) and knockout (KO = ADNP−/−) embryos. The photographs show freshly dissected littermates, ADNP−/− embryos are markedly smaller than the ADNP+/+ embryos, and do not go through axial rotation [taking place under normal conditions on E8.0–E9.5; (Pinhasov et al., 2003)]. (B) Total RNA from two E9 genotype-identical littermates was used on each Affymetrix array (total embryos used = 14, 2 embryos/array, totaling seven arrays). Two distinct clusters of differential gene expression are shown.

overnight at 4 °C in 1 ml binding buffer (0.5% Triton X-100, 1 mM EGTA, 25 mM HEPES pH 7.4, and 75 mM NaCl) with a protease inhibitors cocktail (Sigma St. Louis, MO). Pre-cleared slurry (30 min rotation with beads at 4 °C before antibody addition) was supplemented with protein A/G Plus agarose beads (30 μl; Santa Cruz Biotechnology, Santa Cruz, CA) and the mixture was incubated for 1 h at 4 °C. The protein sample was then subjected to centrifugation at 2000×*g* for 1 min to pellet the beads and the supernatant was removed. The beads were then washed four times with wash buffer (similar to the binding buffer, above), followed by a wash with PBS. Sample-buffer was added to the beads and the samples were boiled for 10 min. Proteins were

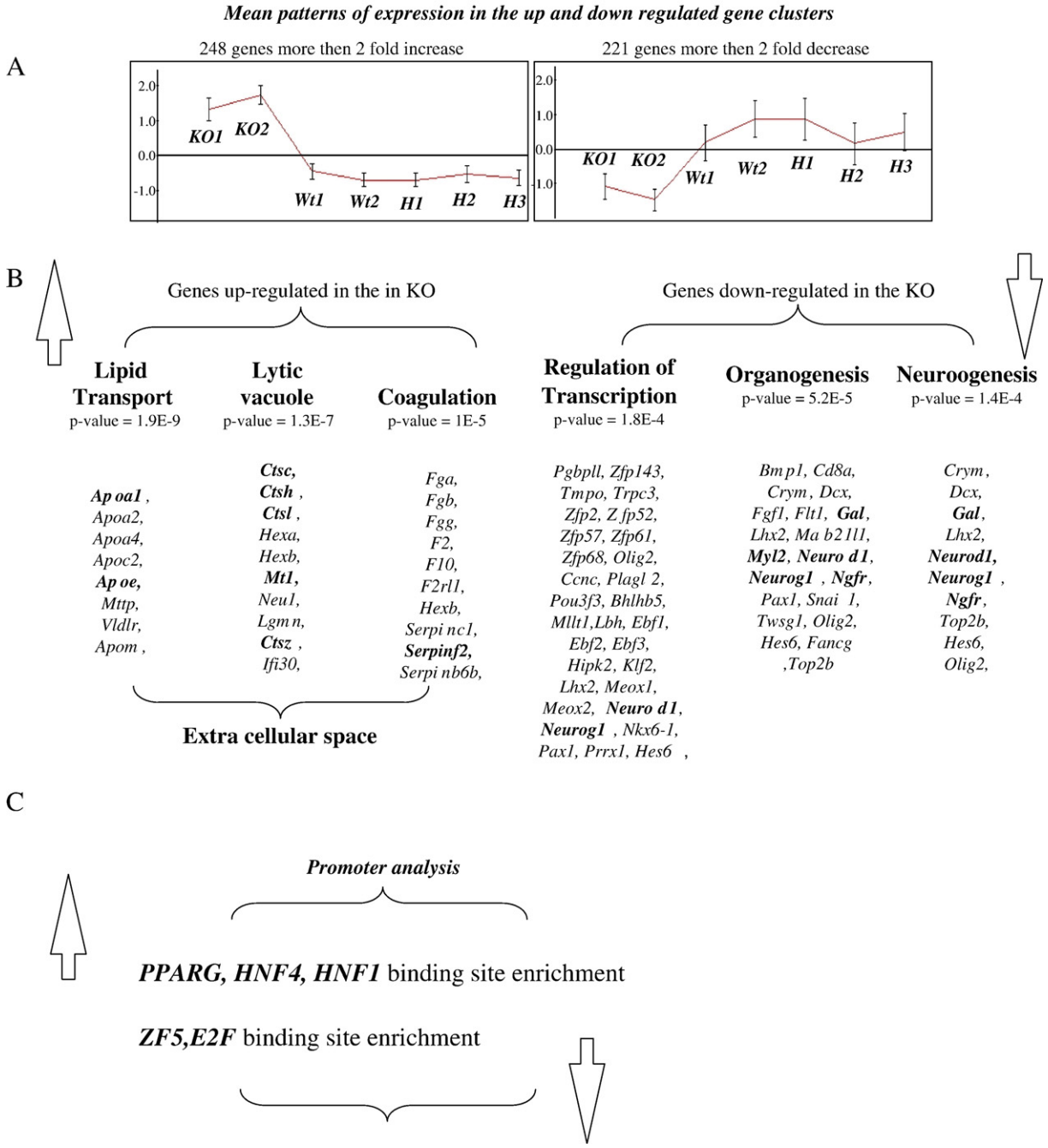

Fig. 2. Patterns of expression and functional/promoter analysis of ADNP KO mice. (A) Only genes that showed >2-fold change in expression as a consequence of ADNP manipulation were further analyzed. The Expander clustering program (http://www.cs.tau.ac.il/~rshamir/expander/ver3Help.html#Clustering) was used to graph the homogeneity of the up-regulated and down-regulated gene clusters. Differences between the knockout (KO–two arrays, Fig. 1), heterozygous (H, three arrays, Fig. 1) and wild type (WT–two arrays, Fig. 1) embryos are shown. (B) Analysis that combines genes with common destiny to generate functional groups was performed (http://www.cs.tau.ac.il/~rshamir/expander/ver3Help.html#Group_Anal). The significance value and the genes constituting the groups are shown. Genes marked in bold showed dramatic changes and were used as group representatives for further analysis (below). (C) The Expander software promoter analysis revealed transcription factors consensus binding sites that were enriched in the two clusters (up or down regulated genes). (D) Complementary DNA from WT and KO ADNP E9 embryos was subjected to QR-PCR and the products were quantified during the linear phase of amplification. Cytoplasmic β-actin (actin) was used as a control gene. The values represent the ratios of ADNP KO/WT gene expression ($n=3$, Student's t-test $^{*}p<0.05$, $^{**}p<0.005$).

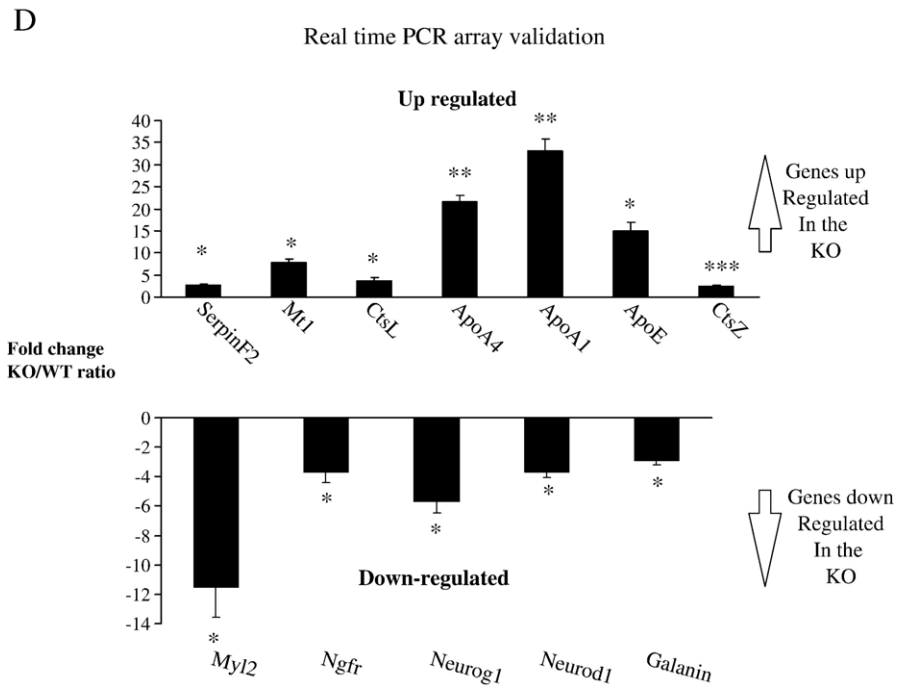

Fig. 2 (*continued*)

separated by sodium dodecyl sulfate–polyacrylamide gel electrophoresis (SDS–PAGE), as described below.

SDS–PAGE and Western analysis

SDS–PAGE for ADNP and HP1α was performed essentially as described (Zamostiano et al., 2001). In brief: proteins (20 μg lane) were separated by electrophoresis on a 10% (w/v) polyacrylamide gel (BioRad, Hercules, CA) containing 0.1% SDS. Molecular weights were determined using Wide Range (6–250 kDa) Multicolored Protein Markers (See Blue, Invitrogen, Carlsbad, CA). The proteins were transferred to PVDF membranes (Invitrogen, Carlsbad, CA) and non-specific antigen sites were blocked using a solution containing 5% non-fat dried milk (w/v) in 10 mM Tris pH 8, 150 mM NaCl and 0.05% Tween 20. Antigen detection was performed using anti Bethyl-ADNP (1:2,000) or anti HP1α (1:1,000).

Antibody–antigen complexes were detected using horseradish peroxidase conjugated secondary protein A (1:5,000, Amersham Biosciences, Buckinghamshire, UK) and visualized by ECL Plus Western blotting detection system (Amersham Biosciences Buckinghamshire, UK).

Results

Gene expression profiling of the ADNP knockout embryo

To identify downstream target genes of ADNP, we examined global gene expression profiles of whole E9 knockout embryos (KO–ADNP$^{-/-}$), their wild-type (WT–ADNP$^{+/+}$) and their heterozygous (H–ADNP$^{-/+}$) littermates, using the Affymetrix Murine Genome 430A oligonucleotide microarrays. E9 embryos were chosen because it is the period by which embryos lacking ADNP exhibit distinct morphological and developmental changes just prior to degeneration and in utero absorption (Fig. 1A). ADNP E9 knockout mouse embryos do not complete axial rotation and neural tube closure. Morphologically, embryonic development of the ADNP knockout mice halts at E8–E8.5. No visible abnormalities were detected in the extra embryonic tissues (visceral yolk sac and amnion). Heterozygous embryos undergo normal embryogenesis, albeit with slight developmental delays (Pinhasov et al., 2003).

Total RNA was extracted from four ADNP knockout embryos, four normal embryos and six heterozygous embryos completely devoid of extra embryonic tissue. A pool of two genotype identical littermates was used on seven different arrays (pooling of two embryos was necessary to obtain sufficient RNA for the microarray analysis). Gene expression results were analyzed using the novel Expander software (Sharan et al., 2003). From the 22,690 probes on the array, only 13,814 showed a significant signal (i.e. were present on the array and showed expression intensity >20 arbitrary units) indicating that these genes were expressed at the E9 stage of embryonic development. The data were normalized using quintiles normalization (Bolstad et al., 2003) in order to remove systematic variation arising from reasons other than biological differences between RNA samples. Data were then analyzed by comparing gene expression levels in the knockout embryos with that of normal and heterozygous embryos (Fig. 1B). Fold change of gene expression levels was used as the filtering criteria for selecting genes of interest. Two sets of gene lists were generated from 469 genes that showed >2 fold change between the ADNP expressing (normal and heterozygous) and the KO embryos, 248, up-regulated genes and 221, down-regulated genes. It is interesting to note that among the 469 genes exhibiting >2 fold change in expression in the ADNP KO embryos, 211 genes showed a distinct differential expression of >3 fold change between the KO embryos and the

rest of the genotypes [SOM algorithm, (Tamayo et al., 1999)] (Fig. 2A).

Functional analysis

Each of the up-regulated and down-regulated gene clusters was analyzed using the Gene Ontology database (Ashburner et al., 2000) to determine significant functional groups within the different clusters (Sharan et al., 2003). Six significant functional groups (P-value $< 10^{-4}$) were generated, three from each cluster (Fig. 2B). The cluster of genes down-regulated in the knockout embryos consisted of the following functional groups: regulation of transcription—genes associated with any process that modulates the frequency, rate or extent of the synthesis of RNA. Organogenesis—genes related to the determination of morphogenesis of a tissue or tissues that work together to perform a specific function. Neurogenesis—genes related to the origin and formation of the nervous tissue. All these key processes were shown to be impaired or delayed in knockout embryos that were devoid of ADNP expression.

The functional groups deduced from the cluster of up-regulated genes in the ADNP knockout embryos showed greater fold changes as compared to the down-regulated genes. Some of these up-regulated transcripts showed ~30 fold higher expression in the KO compared to WT embryos. These up-regulated genes formulate the following functional groups: lipid transport—protein associated with the directed movement of lipids into, out of, within or between cells. Lytic vacuole—vacuoles maintained at an acidic pH which contains degradative enzymes, including a wide variety of acid hydrolases. Coagulation—any process that modulates the frequency, rate or extent of blood coagulation, including proteases and anti-proteases that may be associated with embryogenesis. The three up-regulated sub groups are all included in the functional extracellular space group, consisting of proteins that participate in processes outside the cells and included to a large extent in the visceral endoderm that forms parts of the extra embryonic tissue. Other genes of significance for the visceral endoderm, that are not included in the functional groups cited above, were also up-regulated in the ADNP KO embryos, including, *HNF4 DAB2* (Cammas et al., 2002) *BMP2* (Maye et al., 2000) and *RBP4* (Johansson et al., 1997). The increase in visceral endoderm gene expression in ADNP KO embryos is specific to certain genes and does not include all extra-embryonic tissue genes, thus excluding the possibility of extra embryonic tissue contamination. For example, no significant changes in ADNP KO embryos in comparison to WT embryos were detected in the expression of extra embryonic tissue associated genes such as enolase alfa (*ENO1*), ribosomal protein L13a (*RPL13A*) *HSP70*, cellular nucleic acid binding protein 1 (*CNBP*) (Palis and Kingsley, 1995) and *OTX2* (Maye et al., 2000).

Promoter analysis

Using genomic binding sequences of known transcription factors, it is possible to deduce transcriptional networks and regulatory elements out of gene expression data (Elkon et al., 2003). By calculating the relative occurrence of putative binding sites on promoters of genes, it is possible to deduce specific transcription factors that are significantly enriched in the clusters generated above. The promoters of the genes found to be up-regulated by ADNP-deficiency were also found to be enriched in regulatory elements that interact with the following transcription factors: hepatocyte nuclear factor 1 and 4 (*HNF1, HNF4*) and peroxisome proliferative activated receptor, gamma (*PPARG)*. In contrast, down-regulated genes were enriched in binding sites to *E2F* and *ZF5* transcription factors (Fig. 2C). Interestingly, as indicated above, *HNF4* gene transcripts were found to be up-regulated in the ADNP KO mice.

Microarray data validation

In order to validate the microarray results, quantitative real time polymerase chain reaction (QR-PCR) was performed as described before (Sigalov et al., 2000; Zaltzman et al., 2004). For this purpose, six embryos (E9) were used for RNA extraction, including three wild type (WT, ADNP+/+) and three ADNP knockout embryos (KO, ADNP−/−). Galanin (*gal*), neurogenin1 (*neurog1*) and neuroD1 (*neuroD1)*, genes associated with neurogenesis, organogenesis and transcription control (Fig. 2) that were down-regulated (>2.5-fold) on the array were analyzed by QR-PCR. Results showed that the corresponding transcripts were markedly decreased in the KO mice as compared to the WT. Of the up-regulated genes, apolipoproteinE (*apoE*) and apolipoproteinA1 (*apoA1*) were essentially absent in the WT embryos and highly expressed in the KO mice, while the cathepsin family of enzymes showed a marked increase in the KO as compared to the WT embryos (Fig. 2D). The QR-PCR results are in agreement with the results obtained by microarray analyses. The genes analyzed represent the three major functional groups that are up-regulated as a consequence of ADNP knockout. Expression was normalized relative to actin, a cytoskeletal protein that did not show a significant change in expression as a result of ADNP knockout.

Detecting genes downstream in the ADNP cascade

Genes that showed markedly augmented or reduced expression (>2.5-fold) in the knockout embryos, most likely in response to ADNP deficiency, were considered as potential target genes (PTGs) in the ADNP down stream cascade.

To verify the association of these genes with ADNP during neuronal differentiation, we used the chromatin immunoprecipitation assay (ChIP). This method evaluated the putative direct association between ADNP and a specific PTG. P19, the pluripotent embryonic carcinoma cell line, was selected as a model for this assay. This model cell line was chosen because 1] it has the potential to differentiate into neuronal-like cells, mimicking, in part, the process of neurogenesis; 2] ADNP was originally cloned from an expression library derived from P19 cells (Bassan et al., 1999). Six PTG candidates including the up-regulated apolipoprotein E, cathepsins C, Z and metalotionine 1 and the down-regulated neurogenin 1, and myosin light chain 2

were tested. To evaluate interaction between the PTGs promoters and ADNP in cultured P19 non-differentiated and differentiated cells (treated with retinoic acid) chromatin was extracted and precipitated with antibodies against ADNP. Primers were constructed to the promoter proximal region of the PTG candidates and the DNA derived from the ChIP of the differentiated and non-differentiated P19 cells was assayed for the presence of PTG candidate promoters. Non-immune rabbit serum was used as negative control for the specificity of the antibodies. In the ChIP assay, a PTG is considered positive if the signal from the specific antibody is higher than that of the non-immune control. The efficiency of the PCR primers and the specificity for the correct DNA sequence is demonstrated by the successful amplification of input non-immunoprecipitated DNA (Fig. 3A, Input DNA). The ChIP analysis demonstrated that immunoreactive-ADNP interacted with chromatin that includes all the six PTG promoters tested in differentiated but not in non-differentiated P19 cells (Fig. 3A). Neuronal-like differentiation was induced by retinoic acid and measured by the expression of neuronal-specific genes including neurogenin1, Neurod1 and Tubulinβ3 (Fig. 3B).

ADNP interacts with heterochromatin 1α (HP1α)

The ChIP indicated that ADNP-like immunoreactivity interacts with the chromatin in neuro-differentiated P19 cells. It therefore raised the possibility that ADNP interacts with chromatin binding proteins. Bioinformatics search identified a conserved potential heterochromatin protein1α (HP1α) binding motif PxVxL (Thiru et al., 2004) on human, rat and mouse ADNP (Fig. 4A). HP1α is associated with epigenetic regulation of gene expression through this conserved HP1α binding motif. HP1α is associated with the regulation of transcription trough chromatin interaction with a series of nuclear proteins (Lechner et al., 2005). HP1α participates in chromatin condensation and has a well-established function in heterochromatin-mediated silencing (Eissenberg and Elgin, 2000) that may lead to cellular differentiation (Cammas et al., 2002) and change its degree of

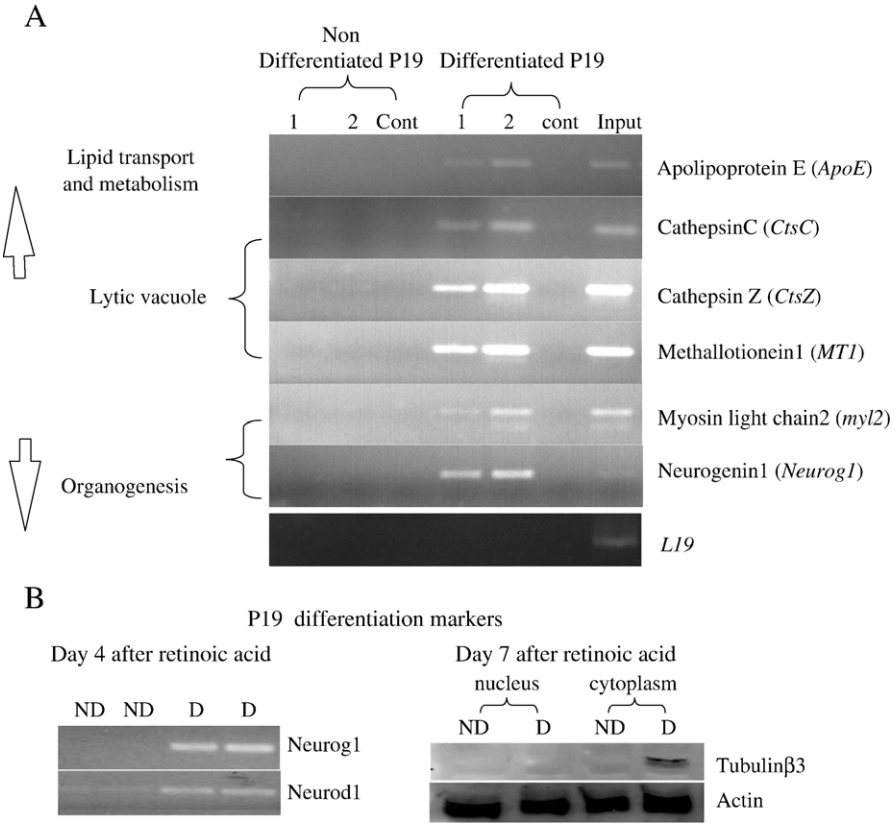

Fig. 3. Chromatin immunoprecipitation of ADNP target gene promoters from differentiated and non-differentiated P19 cells. (A) P19 chromatin immunoprecipitated with anti ADNP (Bethyl) was subjected to PCR amplification, agarose gel electrophoresis and ethidium bromide staining. Gel lanes 1, 2 = immunoprecipitation with ADNP antibody; cont = immunoprecipitation with non-immune antibody; input = chromatin prior to immunoprecipitation. Non-differentiated and differentiated P19 cells (7 days after retinoic acid induction) were used. Each gene lane represents DNA precipitated in one independent experiment (two out of three such experiments are shown, lanes 1 and 2). Similar results were obtained with another ADNP antibody (anti 79) described in Materials and methods). (B) Markers for P19 differentiation: Neurogenin1, Neurod1 transcript detection was performed by PCR followed by agarose gel electrophoresis indicating progress in neuro/glial differentiation (experiments were performed in duplicates as shown in the electropherogram). The expression of the above mentioned proteins was analyzed during differentiation of the P19 cells to neuronal/glial-like cells, 4 days after the addition of retinoic acid. Western analysis of the tubulinβ3 protein (Divinski et al., 2006) in P19 differentiated cytoplasm (7 days after the addition of retinoic acid) indicated that the cell acquired the neuronal cell fate. D—differentiated, ND—non-differentiated.

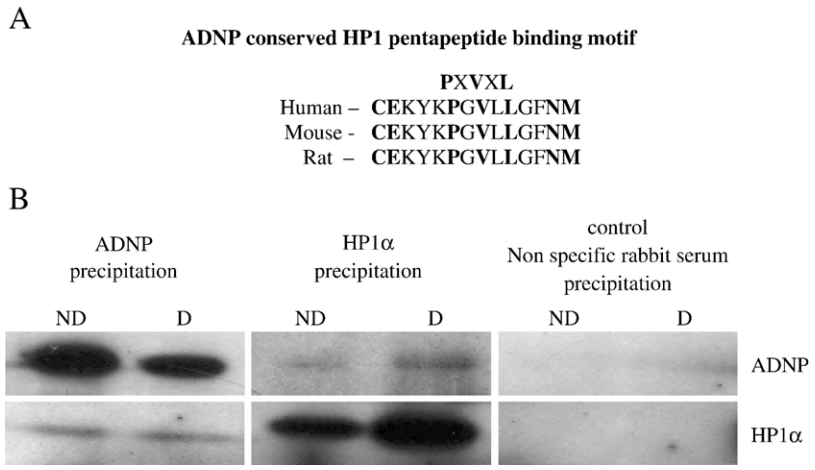

Fig. 4. ADNP interacts with HP1α. (A) Bioinformatic analysis identified a canonical HP1α binding site on ADNP (Thiru et al., 2004). (B) Immunoprecipitation with either ADNP antibodies (mouse monoclonal anti ADNP antibodies, BD Biosciences) or HP1α antibodies (rabbit polyclonal, Sigma) resulted in co-immunoprecipitation of both proteins. Precipitation was preformed on both differentiated (D) P19 and none differentiated (ND) P19 cells. Rabbit non-specific serum was used as specificity Control. The immunoprecipitated proteins were subjected to polyacrylamide gel electrophoresis as described in Materials and methods.

chromatin association (Meshorer et al., 2006). Here, using co-immunoprecipitation on differentiated and non differentiated P19 nuclear protein extracts it was shown that a low amount of HP1 α-like immunoreactivity was recovered after immunoprecipitation with ADNP antibodies and similarly ADNP-like immunoreactivity was recovered after immunoprecipitation with HP1 α antibodies (Fig. 4B). These results suggest that HP1 α may be a binding partner of ADNP. Furthermore, the co-immunoprecipitation assays suggest that ADNP and HP1α co-interact both in differentiated and in non differentiated cells (Fig. 4B).

Discussion

The current study suggests that ADNP is associated with the regulation of multiple gene families during embryonic development. These gene families include: key transcription factors, essential genes associated with neurogenesis/organogenesis, lytic vacuoles and lipid transport. Representative up-regulated genes as a result of ADNP KO included apolipoprotein E, apolipoprotein A1 (~30-fold), metalotionine1 (~8-fold) and cathepsins C, Z (~2–4-fold). Representative down-regulated genes included myosin light chain 2 (~12-fold) and neurogenin1 (~5-fold). ADNP-KO lethality could thus be explained by the massive changes in essential gene expression that impact the development of vital organs including the heart (Huang et al., 2003), the liver (Terasawa et al., 1999) and the nervous system (Pinhasov et al., 2003).

Promoter analysis identified *HNF4* regulatory elements shared by the up-regulated gene transcripts. The *HNF4* gene itself that is known to be associated with hepatic development (hepatic nuclear factor 4) was up-regulated by more then 3 fold as a consequence of ADNP-deficiency.

In view of the above cited findings that imply multiple gene regulation by ADNP during organogenesis, we opted to first study neuronal differentiation in a well defined cell line. Chromatin immunoprecipitation with ADNP antibodies in retinoic acid neuro/glial differentiated P19 cells identified interaction of ADNP with the chromatin containing the above-mentioned specific gene promoters. In contrast, ADNP did not interact with these promoters at the non-differentiated pluripotent stage. These results suggest interaction of ADNP with chromatin proteins that change with cellular differentiation. One candidate binding partner is HP1 α. Taken together, the data obtained strengthen the hypothesis that ADNP is involved either directly or indirectly in the regulation of multiple gene products through chromatin interactions at a crucial point of embryogenesis/neurogenesis.

Gene transcripts up-regulated in the ADNP KO embryos shown to be directly associated with ADNP through the ChIP assay included apolipoproteinE, cathepsinC, cathepsinZ and methallotionein1. These gene products are part of the functional groups of lipid transport and metabolism as well as lytic vacuole

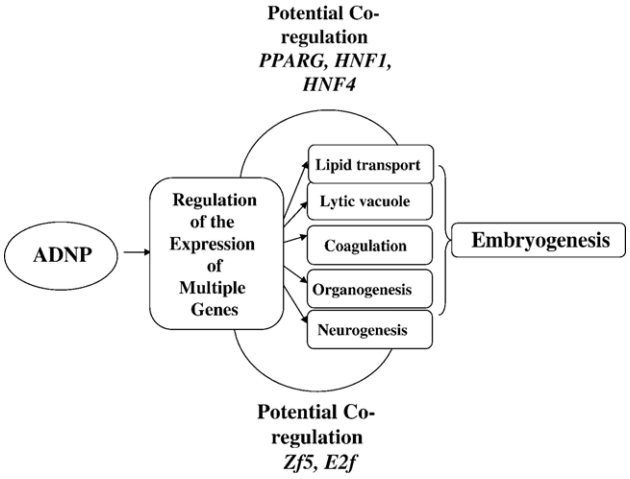

Scheme 1. ADNP regulatory pathways.

activity that constitutes visceral yolk sac/liver-like functions at E7–10 (Palis and Kingsley, 1995; Terasawa et al., 1999). Lipoprotein synthesis and secretion is essential during embryonic development, especially at mid gestation (Terasawa et al., 1999). It has also been established that prior to development of the chorioallentoic placenta, the supply of amino acids to the developing embryo is mediated by the visceral yolk sac (Freeman et al., 1981) and a majority of the amino acids incorporated into embryonic proteins are derived from proteins hydrolyzed in this tissue by cathepsins among other lysosomal proteases (Beckman et al., 1996). The current results indicate that ADNP plays a role in the regulation of genes associated with extra embryonic tissue at the stage of neural tube closure in the developing embryo. We hypothesize that the absence of ADNP that leads to increase in visceral endoderm-associated gene expression contributes to the arrest of embryogenesis/neurogenesis. Interestingly, visceral endoderm can induce anterior epiblast tissue, destined to make neural ectoderm, to differentiate into hematopoietic cells (Belaoussoff et al., 1998). Here, we found that in the absence of ADNP there is an increase in proteins destined to be expressed in the plasma (the extracellular space functional group) (Thomas et al., 1990) implying a mechanism that involves ADNP. In addition, apolipoproteinE and the cathepsin family of proteases have been associated with Alzheimer's disease, with apolipoprotein E4 being a risk factor (Nicodemus et al., 2004) and impaired metabolism of cathepsins may contribute to disease progression (Hook et al., 2005).

The ChIP assay suggests that ADNP is a chromatin binding protein and bioinformatic analysis as well as the co-immunoprecipitation assays indicate that a potential protein binding partner of ADNP is HP1α. HP1α has been associated with cellular differentiation as follows. (1) It has been associated with heterochromatin recruitment in f2 mouse carcinoma cells induced to differentiate into endoderm-like cells by retinoic acid (Cammas et al., 2004). (2) Is the only member of the HP1 family interacting with the centromeric heterochromatin during cell division (Hayakawa et al., 2003). (3) It has been associated with the silencing of *E2F*-target genes (Williams et al., 2003). Here we show that: (1) The expression of *E2F* target genes is decreased in ADNP-deficient mice, and (2) HP1α and ADNP co-immunoprecipitate. It is may be hypothesized that ADNP is associated in part with HP1α chromatin interactions which may influence cell fate and epigenic regulation.

In conclusion, our current data suggest a role for ADNP in a cascade of events that controls embryonal development, with its deletion having effects on neurogenesis/cardiogenesis through suppression of visceral endoderm associated genes (and hepatogenesis) in the developing embryonic body (Scheme 1).

Acknowledgments

We would like to thank Drs. J. Jacob-Hirsch and N. Amariglio, R. Elkon, A. Pinhasov and Ms. I. Vulih-Shultzman for their help. These studies were supported by the US-Israel Binational Science Foundation, the Israel Science Foundation and Allon Therapeutics, Inc.

We also like to thank the Arison family for their donation to the Center of DNA Chips in Pediatric Oncology, Chaim Sheba Medical Center. Prof. G. Rechavi holds the Djerassi Chair in Oncology. Prof. I. Gozes is the incumbent of the Lily and Avraham Gildor Chair for the Investigation of Growth Factors, and heads the Dr. Diana and Zelman Elton (Elbaum) Laboratory for Molecular Neuroendocrinology. Prof. Gozes serves as the Chief Scientific Officer of Allon Therapeutics, Inc.

References

Akiyama, H., Sugiyama, A., Uzawa, K., Fujisawa, N., Tashiro, Y., Tashiro, F., 2003. Implication of Trip15/CSN2 in early stage of neuronal differentiation of P19 embryonal carcinoma cells. Brain Res. Dev. Brain Res. 140, 45–56.

Ashburner, M., Ball, C.A., Blake, J.A., Botstein, D., Butler, H., Cherry, J.M., Davis, A.P., Dolinski, K., Dwight, S.S., Eppig, J.T., Harris, M.A., Hill, D.P., Issel-Tarver, L., Kasarskis, A., Lewis, S., Matese, J.C., Richardson, J.E., Ringwald, M., Rubin, G.M., Sherlock, G., 2000. Gene ontology: tool for the unification of biology. The gene ontology consortium. Nat. Genet. 25, 25–29.

Bassan, M., Zamostiano, R., Davidson, A., Pinhasov, A., Giladi, E., Perl, O., Bassan, H., Blat, C., Gibney, G., Glazner, G., Brenneman, D.E., Gozes, I., 1999. Complete sequence of a novel protein containing a femtomolar-activity-dependent neuroprotective peptide. J. Neurochem. 72, 1283–1293.

Beckman, D.A., Brent, R.L., Lloyd, J.B., 1996. Sources of amino acids for protein synthesis during early organogenesis in the rat: 4. Mechanisms before envelopment of the embryo by the yolk sac. Placenta 17, 635–641.

Belaoussoff, M., Farrington, S.M., Baron, M.H., 1998. Hematopoietic induction and respecification of A–P identity by visceral endoderm signaling in the mouse embryo. Development 125, 5009–5018.

Bolstad, B.M., Irizarry, R.A., Astrand, M., Speed, T.P., 2003. A comparison of normalization methods for high density oligonucleotide array data based on variance and bias. Bioinformatics 19, 185–193.

Cammas, F., Oulad-Abdelghani, M., Vonesch, J.L., Huss-Garcia, Y., Chambon, P., Losson, R., 2002. Cell differentiation induces TIF1beta association with centromeric heterochromatin via an HP1 interaction. J. Cell Sci. 115, 3439–3448.

Cammas, F., Herzog, M., Lerouge, T., Chambon, P., Losson, R., 2004. Association of the transcriptional corepressor TIF1beta with heterochromatin protein 1 (HP1): an essential role for progression through differentiation. Genes Dev. 18, 2147–2160.

Chen, S.Y., Charness, M.E., Wilkemeyer, M.F., Sulik, K.K., 2005. Peptide-mediated protection from ethanol-induced neural tube defects. Dev. Neurosci. 27, 13–19.

Divinski, I., Holtser-Cochav, M., Vulih-Schultzman, I., Steingart, R.A., Gozes, I., 2006. Peptide neuroprotection through specific interaction with brain tubulin. J. Neurochem. 98, 973–984.

Eissenberg, J.C., Elgin, S.C., 2000. The HP1 protein family: getting a grip on chromatin. Curr. Opin. Genet. Dev. 10, 204–210.

Elkon, R., Linhart, C., Sharan, R., Shamir, R., Shiloh, Y., 2003. Genome-wide in silico identification of transcriptional regulators controlling the cell cycle in human cells. Genome Res. 13, 773–780.

Freeman, S.J., Beck, F., Lloyd, J.B., 1981. The role of the visceral yolk sac in mediating protein utilization by rat embryos cultured in vitro. J. Embryol. Exp. Morphol. 66, 223–234.

Furman, S., Steingart, R.A., Mandel, S., Hauser, J.M., Brenneman, D.E., Gozes, I., 2004. Subcellular localization and secretion of activity-dependent neuroprotective protein in astrocytes. Neuron Glia Biol. 1, 193–199.

Gozes, I., 2001. Neuroprotective peptide drug delivery and development: potential new therapeutics. Trends Neurosci. 24, 700–705.

Gozes, I., Zamostiano, R., Pinhasov, A., Bassan, M., Giladi, E., Steingart, R.A., Brenneman, D.E., 2000. A novel VIP responsive gene. Activity dependent neuroprotective protein. Ann. N. Y. Acad. Sci. 921, 115–118.

Gozes, I., Morimoto, B.H., Tiong, J., Fox, A., Sutherland, K., Dangoor, D., Holser-Cochav, M., Vered, K., Newton, P., Aisen, P.S., Matsuoka, Y., van Dyck, C.H., Thal, L., 2005. NAP: research and development of a peptide

derived from activity-dependent neuroprotective protein (ADNP). CNS Drug Rev. 11, 353–368.

Greene, N.D., Leung, K.Y., Wait, R., Begum, S., Dunn, M.J., Copp, A.J., 2002. Differential protein expression at the stage of neural tube closure in the mouse embryo. J. Biol. Chem. 277, 41645–41651.

Gressens, P., Hill, J.M., Gozes, I., Fridkin, M., Brenneman, D.E., 1993. Growth factor function of vasoactive intestinal peptide in whole cultured mouse embryos. Nature 362, 155–158.

Hayakawa, T., Haraguchi, T., Masumoto, H., Hiraoka, Y., 2003. Cell cycle behavior of human HP1 subtypes: distinct molecular domains of HP1 are required for their centromeric localization during interphase and metaphase. J. Cell Sci. 116, 3327–3338.

Hill, J.M., Glazner, G.W., Lee, S.J., Gozes, I., Gressens, P., Brenneman, D.E., 1999. Vasoactive intestinal peptide regulates embryonic growth through the action of activity-dependent neurotrophic factor. Ann. N. Y. Acad. Sci. 897, 92–100.

Hombria, J.C., Lovegrove, B., 2003. Beyond homeosis–HOX function in morphogenesis and organogenesis. Differentiation 71, 461–476.

Hook, V., Toneff, T., Bogyo, M., Greenbaum, D., Medzihradszky, K.F., Neveu, J., Lane, W., Hook, G., Reisine, T., 2005. Inhibition of cathepsin B reduces beta-amyloid production in regulated secretory vesicles of neuronal chromaffin cells: evidence for cathepsin B as a candidate beta-secretase of Alzheimer's disease. Biol. Chem. 386, 931–940.

Huang, C., Sheikh, F., Hollander, M., Cai, C., Becker, D., Chu, P.H., Evans, S., Chen, J., 2003. Embryonic atrial function is essential for mouse embryogenesis, cardiac morphogenesis and angiogenesis. Development 130, 6111–6119.

Johansson, S., Gustafson, A.L., Donovan, M., Romert, A., Eriksson, U., Dencker, L., 1997. Retinoid binding proteins in mouse yolk sac and chorio-allantoic placentas. Anat. Embryol. (Berl.) 195, 483–490.

Lechner, M.S., Schultz, D.C., Negorev, D., Maul, G.G., Rauscher III, F.J., 2005. The mammalian heterochromatin protein 1 binds diverse nuclear proteins through a common motif that targets the chromoshadow domain. Biochem. Biophys. Res. Commun. 331, 929–937.

Maye, P., Becker, S., Kasameyer, E., Byrd, N., Grabel, L., 2000. Indian hedgehog signaling in extraembryonic endoderm and ectoderm differentiation in ES embryoid bodies. Mech. Dev. 94, 117–132.

Meshorer, E., Yellajoshula, D., George, E., Scambler, P.J., Brown, D.T., Misteli, T., 2006. Hyperdynamic plasticity of chromatin proteins in pluripotent embryonic stem cells. Dev. Cell 10, 105–116.

Nicodemus, K.K., Stenger, J.E., Schmechel, D.E., Welsh-Bohmer, K.A., Saunders, A.M., Roses, A.D., Gilbert, J.R., Vance, J.M., Haines, J.L., Pericak-Vance, M. A., Martin, E.R., 2004. Comprehensive association analysis of APOE regulatory region polymorphisms in Alzheimer disease. Neurogenetics 5, 201–208.

Palis, J., Kingsley, P.D., 1995. Differential gene expression during early murine yolk sac development. Mol. Reprod. Dev. 42, 19–27.

Pinhasov, A., Mandel, S., Torchinsky, A., Giladi, E., Pittel, Z., Goldsweig, A.M., Servoss, S.J., Brenneman, D.E., Gozes, I., 2003. Activity-dependent neuroprotective protein: a novel gene essential for brain formation. Brain Res. Dev. Brain Res. 144, 83–90.

Poggi, S.H., Vink, J., Goodwin, K., Hill, J.M., Brenneman, D.E., Pinhasov, A., Gozes, I., Spong, C.Y., 2002. Differential expression of embryonic and maternal activity-dependent neuroprotective protein during mouse development. Am. J. Obstet. Gynecol. 187, 973–976.

Rozen, S., Skaletsky, H., 2000. Primer3 on the WWW for general users and for biologist programmers. Methods Mol. Biol. 132, 365–386.

Sharan, R., Maron-Katz, A., Shamir, R., 2003. CLICK and EXPANDER: a system for clustering and visualizing gene expression data. Bioinformatics 19, 1787–1799.

Sigalov, E., Fridkin, M., Brenneman, D.E., Gozes, I., 2000. VIP-Related protection against lodoacetate toxicity in pheochromocytoma (PC12) cells: a model for ischemic/hypoxic injury. J. Mol. Neurosci. 15, 147–154.

Steingart, R.A., Gozes, I., 2006. Recombinant activity-dependent neuroprotective protein protects cells against oxidative stress. Mol. Cell. Endocrinol. 252, 148–153.

Tamayo, P., Slonim, D., Mesirov, J., Zhu, Q., Kitareewan, S., Dmitrovsky, E., Lander, E.S., Golub, T.R., 1999. Interpreting patterns of gene expression with self-organizing maps: methods and application to hematopoietic differentiation. Proc. Natl. Acad. Sci. U. S. A. 96, 2907–2912.

Terasawa, Y., Cases, S.J., Wong, J.S., Jamil, H., Jothi, S., Traber, M.G., Packer, L., Gordon, D.A., Hamilton, R.L., Farese Jr., R.V., 1999. Apolipoprotein B-related gene expression and ultrastructural characteristics of lipoprotein secretion in mouse yolk sac during embryonic development. J. Lipid Res. 40, 1967–1977.

Thiru, A., Nietlispach, D., Mott, H.R., Okuwaki, M., Lyon, D., Nielsen, P.R., Hirshberg, M., Verreault, A., Murzina, N.V., Laue, E.D., 2004. Structural basis of HP1/PXVXL motif peptide interactions and HP1 localisation to heterochromatin. EMBO J. 23, 489–499.

Thomas, T., Southwell, B.R., Schreiber, G., Jaworowski, A., 1990. Plasma protein synthesis and secretion in the visceral yolk sac of the fetal rat: gene expression, protein synthesis and secretion. Placenta 11, 413–430.

Wells, J., Farnham, P.J., 2002. Characterizing transcription factor binding sites using formaldehyde crosslinking and immunoprecipitation. Methods 26, 48–56.

Williams, L., Zhao, J., Morozova, N., Li, Y., Avivi, Y., Grafi, G., 2003. Chromatin reorganization accompanying cellular dedifferentiation is associated with modifications of histone H3, redistribution of HP1, and activation of E2F-target genes. Dev. Dyn. 228, 113–120.

Zaltzman, R., Alexandrovich, A., Beni, S.M., Trembovler, V., Shohami, E., Gozes, I., 2004. Brain injury-dependent expression of activity-dependent neuroprotective protein. J. Mol. Neurosci. 24 (2), 181–187.

Zamostiano, R., Pinhasov, A., Gelber, E., Steingart, R.A., Seroussi, E., Giladi, E., Bassan, M., Wollman, Y., Eyre, H.J., Mulley, J.C., Brenneman, D.E., Gozes, I., 2001. Cloning and characterization of the human activity-dependent neuroprotective protein. J. Biol. Chem. 276, 708–714.

Zusev, M., Gozes, I., 2004. Differential regulation of activity-dependent neuroprotective protein in rat astrocytes by VIP and PACAP. Regul. Pept. 123, 33–41.